On the Suitability of Using Halbach Arrays as Potential Energy Storage Media

Daniel Månsson*

Abstract—In the work presented here, the suitability of an unusual energy storage medium is investigated. The energy storage system is based on the forceful compression of two magnetic Halbach arrays. The mass and volume energy density is obtained and compared to existing common energy storage systems. The charge and discharge times and depths are also discussed. In addition, limits and considerations, which are needed for practical implementation, e.g., risk of demagnetization, internal mechanical stresses, heating of the magnetic structure and financial efficiency are investigated.

1. INTRODUCTION

The threat of global warming and diminished resources is today a growing concern. It leads to the conclusion of effective use of energy, on all levels of society, as the most vital point. Thus, to increase the effectiveness of society's energy utilization, the idea of the "smart electricity grid" has been suggested and is internationally recognized and investigated. The key concepts of these smart grids are based around ICT, distributed generation and energy storage. This means that traditional large power generation will be supplemented with, e.g., wind, solar and other renewable energy sources whose production is distributed over the geographical area of concern. However, these renewable energy sources are stochastic and, thus, the peak energy availability in, e.g., the solar intensity, may not coincide with the peak energy demand. Therefore, the energy produced must be stored in an intermediary state in wait for the demand to increase. The stored energy can be in the form of chemical energy in batteries, potential energy of elevated water in a basin, electromagnetic energy in the charge of a capacitor, kinetic energy in the momentum of a flywheel etc. (see e.g., [1–3]).

In addition to this comes the concept of the "prosumer" (i.e., producer-consumer) [4]. An example of this is a residential home with renewable energy production (e.g., through wind or solar power) with an energy storage system that can store, and return to the grid, surplus energy that is currently not in demand locally. The local energy demand is obtained through "smart meters" [5] and other measurements of the power consumed locally in devices and equipment. This information is used to determine the surplus, or deficit, of power available locally where a surplus can be returned to the grid. In addition, it is important to realize that energy storage systems act as stabilizers in the grid and can, e.g., support a strained generation if the load is high. Many financial schemes for energy return or small scale energy production is discussed and tested around the globe today.

A fundamental, but crucial, point for the prosumer is that there is a reliable, safe and, both electrotechnical and financially, effective method of storing the energy in an intermediate form to balance the produced energy surplus or deficit. Large scale energy storage has already existed for a relatively long time in power grids, often in the form of elevated water in a basin (so called pumped hydro storage). More recently more novel methods with, e.g., compressed air energy storage (CAES), large arrays of

flywheels or superconducting magnets as the storage media have been investigated and/or introduced. An energy storage system can operate in three different states; charging, storing or discharging and some important parameters when investigating and comparing different media are:

- Energy storage capability (both volume energy density [J/m^3] and weight energy density [J/kg]).
- Charge/discharge times ([s]).
- Charge/discharge depth ([%]).
- Unit energy stored per capital cost (e.g., [J/USD]).
- Conversion losses.

It is important, for the successful implementation of all aspects of the smart grid, to evaluate unusual forms of energy storage media and systems. This as all types of energy storage will not be equally suitable for all applications and installations in a smart grid. The needs and requirements of the energy storage system (e.g., energy density, charge/discharge times, charging/discharging depth etc.) will differ both with the production method used (e.g., photovoltaic cells versus wind power plant) but also with the characteristic of the load (e.g., residential homes compared to apartment buildings).

NdFeB (Nd$_2$Fe$_{14}$B) magnets are widely used today for a wide variety of purposes and some commercial types have an adhesive force of approximately 100 kg even though the dimensions are only $5*5*2.5$ cm and for a smaller unit of $1*1*1$ cm the force could be almost 4 kg [6]. Thus, the idea of using permanent magnets as springs and, therefore, as a medium for energy storage is not inconceivable.

There exist, at the time of writing, at least one patent [7] describing a device that utilizes the potential energy stored when simple magnets are forced together. Thus, the aim of this paper is to study the suitability (not the actual implementation!) of a system based on magnetic structures, to be used as a potential energy storage medium in a smart grid/prosumer situation. Several factors, such as the potential energy stored, charge/discharge times, mechanical and other limits and considerations as well as economic suitability are investigated and discussed here.

In the investigations presented here the free software *FEMM* [8] ("Finite element method magnetics") was used and it has previously shown itself to be an accurate tool [9]. However, as with all numerically simulated results the finer details of the quantities (i.e., here the magnetic flux densities, B-fields) are always associated with errors due to, e.g., mesh size and/or the method being used. Also it should be mentioned that FEMM only offers a "2.5D approach (i.e., not "true" 3D). This means that, e.g., the calculated energy in the fields do not include edge effects in the "depth dimension", but does take the depth of the structure into account for the total energy value. In addition, the general field structures, and results, were confirmed (but not shown here) with another field simulation software [10].

The reason that a numerical simulation tool (instead of analytical methods with, e.g., the Maxwell stress tensor) is mainly used in the analysis here is that it is easier to handle, e.g., complicated structures and fields as well as material properties.

2. POTENTIAL ENERGY STORAGE VIA MECHANICAL COMPRESSION

From *Hooke's law*, a compressed spring stores potential energy (barring mechanical deformation in the spring) equivalent to the amount of work carried out against the force from the spring ($F = -kx'$) along the path of compression, C (from point 0 to point x):

$$E_{stored} = -\int_C F dx' = \int_0^x (kx')dx' = \frac{1}{2}x^2. \tag{1}$$

Analogous to the mechanical spring, it requires an amount of work to force two magnets with opposite magnetization direction ($m\hat{n}$ and $-m\hat{n}$) together along the direction of $\hat{n}$ (normal vector to the plane of the magnets). Thus, if a magnet with magnetic moment $-m\hat{z}$ is placed in a magnetic field, with magnetic flux density $\bar{B}$, the potential energy of the configuration becomes [11]:

$$U = -\bar{m} \cdot \bar{B} \tag{2}$$

(the energy needed to maintain the B-field is neglected). The resulting force on the element is:

$$\bar{F} = \nabla(\bar{m} \cdot \bar{B}). \tag{3}$$

For example, if two magnets (approximated as magnetic dipoles with magnetic moment $\bar{m}_1 = -m\hat{z}$ and $\bar{m}_2 = m\hat{z}$) are brought together (see Fig. 1) along the z-axis (m_1 at distance d above m_2) where the magnetic flux density from m_2 becomes (along the z-axis):

$$\bar{B}_2 = \frac{\mu_0 m}{4\pi r^3}\left(2\cos\theta\hat{r} + \sin\theta\hat{\theta}\right)\Big|_{\begin{cases} \theta = 0 \\ r = d \\ \hat{r} = \hat{z} \end{cases}} = \frac{\mu_0 m}{2\pi d^3}\hat{z}, \tag{4}$$

the potential energy stored in the configuration is then:

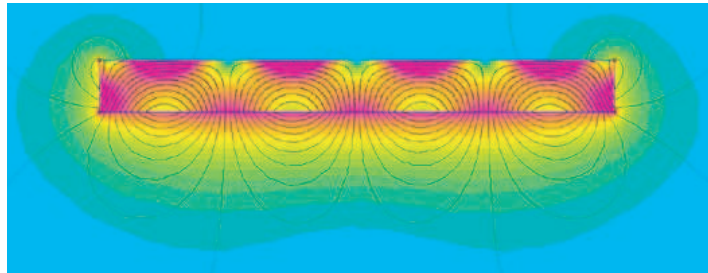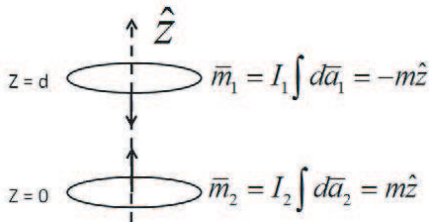$$U = -\bar{m}_1 \cdot \bar{B}_2 = \frac{\mu_0 m^2}{2\pi d^3}. \tag{5}$$

Figure 1. Shown is two dipoles a distance d from each other along the z-axis. The direction of the currents circulating in the loops (and thus the area element and magnetic moment) is derived using the right-hand rule.

Figure 2. Shown is a structure with continuous rotating magnetization directing leading to Halbach arrays (simulated using the FEMM software).

(This approach is not valid if d is small compared to the dimensions of the dipoles.) This is however not an optimal situation as not all of the magnetic flux density from a magnet is involved in the energy storage (mechanical compression of the magnets) as the B-field can be considered to be isotropic. It would be better if the flux densities from the magnets could be concentrated on one side as in a *Halbach array*.

3. HALBACH ARRAYS

3.1. Introduction

The configuration of magnets that is known today as *Halbach arrays* was first described and explained in 1973 by J. C. Mallinson [12] but the name is derived from the later work of Klaus Halbach [13]. Halbach arrays are today used in, e.g., maglev trains, linear generators, and as "wigglers" (in free electron lasers and particle accelerators). Fundamentally, a Halbach array is the result of a particular orientation scheme for the magnetization direction along the magnetic structure.

When employed in a volume (or with individual magnets) the magnetic flux density is canceled on one side of the structure whereas the flux is augmented on the other side (not to be confused with "magnetic monopoles"). For example, for a large planar structure with thickness d lying in the xz-plane with the magnetization in the x and y direction given by [12] (magnetization in z direction is either constant or zero):

$$M_x = M_0 \sin(kx), \quad M_y = M_0 \cos(kx), \quad M_z = 0, \tag{6}$$

the resulting flux (here $|B|$) is shown in Fig. 2.

Analytical expressions for the magnetic flux density on the so called enhancing side can be found in [14] based on [13] but observe the complete expression given in [12].

If discrete magnets are used, and if the magnetization direction is rotated 90° between subsequent magnets, the same result can be approximately reproduced (compare Fig. 2 and Fig. 3 but keep in

mind that the degree of meshing in the simulation will affect the finer structures of the flux). A finer discretization (lower rotation angle) gives a better approximation of the flux density from the continuous Halbach array (Fig. 2) but also leads to thinner individual magnets. In Appendix (see Fig. A1 and Fig. A2) it is seen that a difference in magnetization direction of approximately 22° between subsequent magnets gives a good approximation. I.e., the vector components of the flux densities from a discretized and continuous Halbach array are then approximately equivalent. The magnets in a discretized Halbach array will however experience internal forces between the magnets and have to be fixed in place by, e.g., adhesives (see Section 5.3).
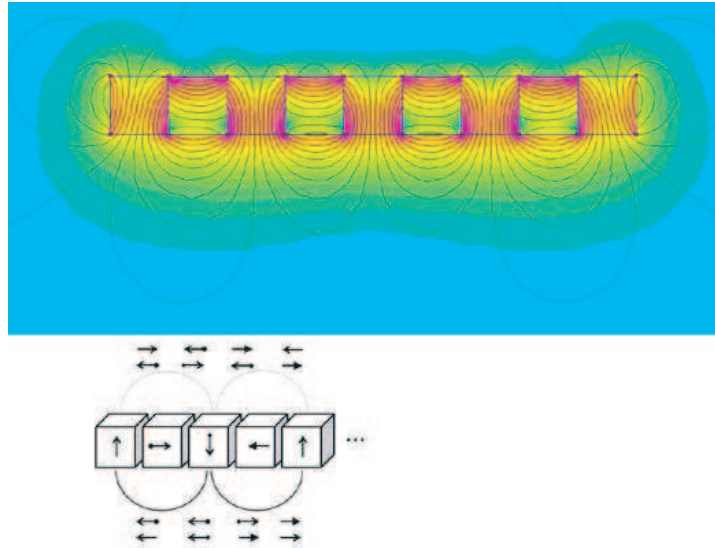

Figure 3. A discretized Halbach array consisting of individual magnets ($1 * 1 * 1$ cm) simulated in FEMM (top) and conceptual drawing showing the cancelation and augmentation of the magnetic flux densities (bottom). Notice that compared to the structure in Fig. 2 the flux on the top-side of the array is less negated.

3.2. Halbach Arrays as Energy Storage Media

Potential energy can be stored if two magnetic structures, with opposing magnetic moment, are forced together. The main advantage of using magnets for energy storage is the absence of degradation in the magnets (if the surrounding environment (e.g., temperature and surrounding magnetic field) is kept within tolerance levels, see Section 5). They will continue to operate as energy storage medium virtually indefinitely, although surrounding auxiliary devices (e.g., motor/generator, mechanical fixtures etc.) will, to the same extent as in other energy storage systems, suffer degradation.

Halbach arrays are optimal for energy storage via mechanical compression of magnetic structures as they have (ideally) a one-sided flux. In addition, such an energy storage system has the ability to, relatively, instantaneously store and release the energy. As we shall see in Section 5 the inherent limitation of the medium on, e.g., the charging time is negligible. The energy will be stored as potential energy as soon as the Halbach arrays have been pressed together. The limit is predominately on the motors, performing the compression (i.e., limit on axillary equipment) as opposed to, e.g., a flywheel where the tensile strength of the material sets limits on the stored energy and charging time (i.e., limit on the medium itself, see Section 5). The charge and discharge depths are considered to be good as the magnets, ideally, do not change between cycles.

For energy storage purposes several units of dual Halbach arrays can be employed in a stacked configuration. The configuration can be such that the units are connected in series or in parallel. In addition, surrounding the units with a material, e.g., Iron, with high permeability would decrease the efficiency of the energy storage ability. This is as a material, e.g., iron, with a high reluctance will increase the magnetic flux in that region, as opposed to without the material. Thus, more of the flux

takes the path in the iron and the result is that the vertical force needed for compression decreases (i.e., the energy storage ability decreases) whereas the horizontal component of the force increases (not shown here). If however, there is a need to limit the fields surrounding the device, this might still be a solution. Other conducting materials (e.g., copper) that do not have a large permeability could be used as support.

4. ANALYSIS OF POTENTIAL ENERGY STORAGE WITH HALBACH ARRAYS

Figure 4 shows two Halbach arrays (with the dimensions; length = 5 cm, height = 1 cm and depth = 1 cm) 1 cm apart. The grade of the NdFeB material used here is approximately "N42 graded". The designation for different NdFeB grades gives a hint of the "quality" of the material, in the sense of energy density (numbering, here "42") and maximum working temperature (lettering, here "N"). The equivalent current source density of the permanent magnet was set in FEMM to approximately 1.03 MA/m (giving a magnetic flux density of approximately 1.3 T). The relative permeability of the material was set to 1.05 in FEMM (following the material parameters in [15]).

For the simulations results presented here the size of the mesh elements, for the magnetic structures, were constrained, through the mesh parameter in FEMM, such that the sides of the triangles of the mesh were no larger than 100 μm. This to assure that the magnetic flux density, for the smallest gap distance chosen (250 μm) is accurately depicted. Finer meshing was tested but did not measurably improve the simulation results.

As described in the introduction, work is required to bring two magnetic structures, with opposite direction of magnetic moment, together. In Fig. 4 two continuous Halbach arrays with the magnetic flux density on opposite sides (and opposing directions) are shown. The rotation rate of the magnetization direction (i.e., magnetic moment, $\bar{m}$) was such that $\bar{m}$ completed one full turn over the length of the array (compare bottom figure of Fig. 3). I.e., the *wave length* (distance between maxima in B-field) is $L/2$ (here 2.5 cm).
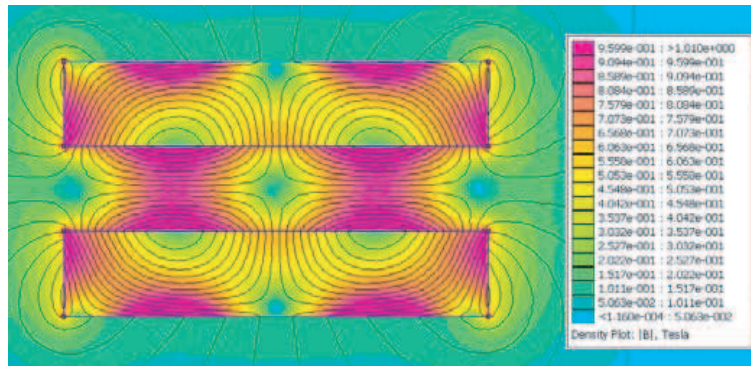

Figure 4. Shown is a dual unit consisting of two continuous Halbach arrays with magnetization such that the majority of the magnetic flux density is concentrated in the gap between them.

To maximize the energy stored in the configuration, the work that is needed to force the magnets together should be maximized (i.e., maximize the path integral, along the compression, of the force).

Figure 5 shows how the force on the top magnet varies (the bottom magnet remains fixed) with the gap distance for different wave lengths. (The term "pole pitch", i.e., the distance between the maxima (poles) in the magnetic flux density is sometime used in the literature.) The path integral (i.e., the work) is taken from, essentially, infinity (even though the force drops to zero much before this) to the chosen stopping distance. As stated above, the stopping distance is here chosen to be 250 μm to avoid erroneous results from the simulations (as the meshing cannot be improved indefinitely without having unreasonable long simulation runtimes). The required work changes with the wave length (see Table 1) and it was seen that for a wave length of "length/2" (here 2.5 cm) the work required to decrease the gap from 5 cm to 250 μm is maximized and, thus, also the stored potential energy is also.

Table 1. The energy stored during compression as a function of the wave length of the two Halbach arrays discussed.

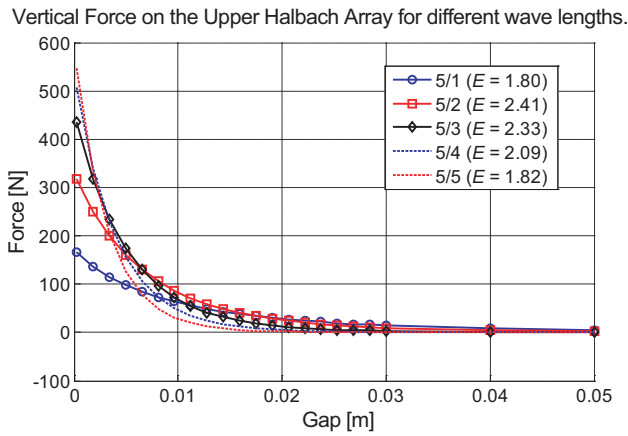| Wave length [cm]	Energy stored [J]
1 ($L/5$)	1.82
1.25 ($L/4$)	2.09
≈ 1.67 ($L/3$)	2.33
2.5 (L/2)	**2.41**
5 ($L/1$)	1.80

Figure 5. Shown are the vertical forces between two continuous Halbach arrays for different wave lengths. As the length (here $L = 5$ cm) is kept constant, a smaller wave length means a higher rotation rate of the angle of magnetization direction. The energy stored (denoted "E") during compression is also shown for the different cases (see also Table 1).
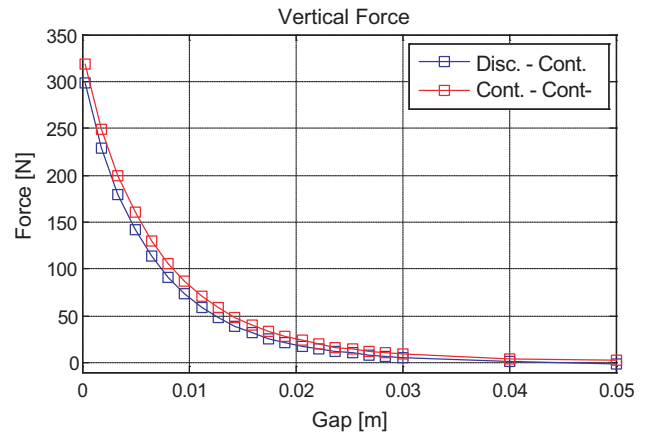
Figure 6. A small difference, in the vertical force between the Halbach arrays, is seen if one of the rows of magnets is exchanged with a discretized Halbach array. This is, in part due, to the losses due to a "leakage flux" on the backside of the discretized Halbach array (compared to the continuous Halbach array). This is however within the reasonable error due to the FEM simulations.

This dependency, on the wave length in the work done, is also seen in [16] where the vertical force on a current carrying structure is maximized for a particular wave length of the Halbach array positioned below (actual value is indirectly dependent on the dimensions of the magnets) and, thus, the work performed is maximized for a particular wave length. This can also be investigated (but not done here) by utilizing the Maxwell stress tensor [17] to calculate the forces involved for different wave lengths.

The total volume of the two magnetic structures that stores the potential energy (ten NdFeB magnets $1\,\mathrm{cm}^3$) is $1 * 10^{-5}\,\mathrm{m}^3$ and the density of the NdFeB material is [15] $7.6 * 10^3\,\mathrm{kg/m}^3$. Thus, the volume and mass energy density is (for a wave length of $L/2$) $241\,\mathrm{kJ/m}^3$ and $32\,\mathrm{J/kg}$, respectively. This volume energy density is close to the maximum energy product (i.e., maximum amount of energy stored in a magnet with an equal volume), given by the manufacturer [6], which states a $(B \times H)_{\mathrm{max}}$ of 318–$334\,\mathrm{kJ/m}^3$ for the N42-graded material. The difference is believed to be due the fact that, even for Halbach arrays, not all of the magnetic flux density in the volume is involved in the compression (as can be seen in Fig. 4). I.e., there exist "side-lobes" that do not increase the force between the magnets, but also that the magnetic structures were compressed to a non-zero gap distance.

5. CONSIDERATIONS AND LIMITATIONS

5.1. Demagnetization Risk

For a very small gap distance ($250\,\mu$m) between the Halbach arrays the magnetic field inside the individual magnets can be quite large. For the magnets studied here, the magnetic field, in some small regions of the corners of some of the individual magnets, reached a value of $\approx 1.2\,$MA/m.

When magnets are exposed to magnetic fields above a critical values they lose, either temporary or permanently, their magnetic properties. The coercivity is a measure of how well magnets can withstand an external field without losing their magnetization. For N-type graded NdFeB the coercivity is $\geq 955\,$kA/m [6] and is larger for other types of NdFeB grades. For example, UH-graded NdFeB has a coercivity of $\geq 1990\,$kA/m and EH-graded has a coercivity of $\geq 2388\,$kA/m. (In addition, higher graded materials have a higher maximum operational temperature ($80°$C for N-type graded material compared to $180°$C and $200°$C for UH- and EH-graded material, respectively).) Thus, for the energy storage medium discussed here, proper choice of NdFeB graded material might be needed but not problematic. This as equivalent energy densities can be found in the higher graded NdFeB materials (e.g., both EH35 (263–$279\,$kJ/m^3) and UH42 (318–$334\,$kJ/m^3) exist with suppliers).

5.2. Effect of Discretization on the Stored Energy

The manufacturing of a structure with continuously rotating magnetization direction is not trivial. Thus, a discretized array (as in Fig. 3) has to be used. Comparing the Halbach array with a continuously changing magnetization direction (wave length of $L/2$) with the equivalent discretized Halbach array consisting of five individual, identical, magnets (with $90°$ rotation of the magnetic moment for consecutive magnets) a small difference is seen. Fig. 6 shows the force on the upper (continuous) Halbach array when the lower one is either continuous or discretized. Only a small difference in the force normal to the surface is seen, even though the discretization is coarse ($90°$ rotation of magnetization direction between subsequent magnets).

Also, for the discretized Halbach array additional design parameters have to be taken into account. In [18] it was shown that the vertical force on a (superconducting) structure (created by a discretized Halbach array) is maximized if consecutive magnets in the Halbach array have of the same width. If the ratio of the widths of two consecutive magnets was larger, or smaller than one, the vertical force was diminished. (Here, in this paper, the widths of consecutive magnets are always all equal.) Thus, the magnetic moments created (in the individual magnets) are equal, but rotated, when the magnetization of the material is rotated (e.g., $90°$) (i.e., normal to the surface of the magnet). Also if the dimensions are not the same, e.g., as in a thin rectangular slab, the magnetic moment varies with the direction of the magnetization in the material. (Actually, only in a sphere is the magnetic moment equal for all directions of magnetization in the material.)

5.3. Mechanical Stresses

5.3.1. Internal Forces in a Discretized Halbach Array

When the gap distance between two discretized Halbach arrays is decreased the individual magnets will experience different vertical and horizontal forces. These internal forces consists of self-forces (i.e., from the other magnets in the same Halbach array) and external forces (i.e., from the other Halbach array). In the situations studied here the sum of the horizontal forces equates to zero, but the adhesive glue holding individual magnets together has to withstand them. The total vertical force is equal to the repellent force shown earlier, e.g., in Fig. 5 or Fig. 6. Notice the symmetry (as also seen in [19]) for the horizontal forces and the similarities in the vertical forces for the two outermost magnets ("Magnet 1" and "Magnet 4") and also between the next outermost magnets ("Magnet 2" and "Magnet 3"). Thus, for practical uses, they have to be fixed in place. The forces, vertical and horizontal, will here reach a maximum magnitude value of approximately $10\,$N and $150\,$N, respectively. These values are not problematic for existing adhesives (which can easily maintain hundreds of kg/cm^2 (thousands of N/cm^2 at sea level)).
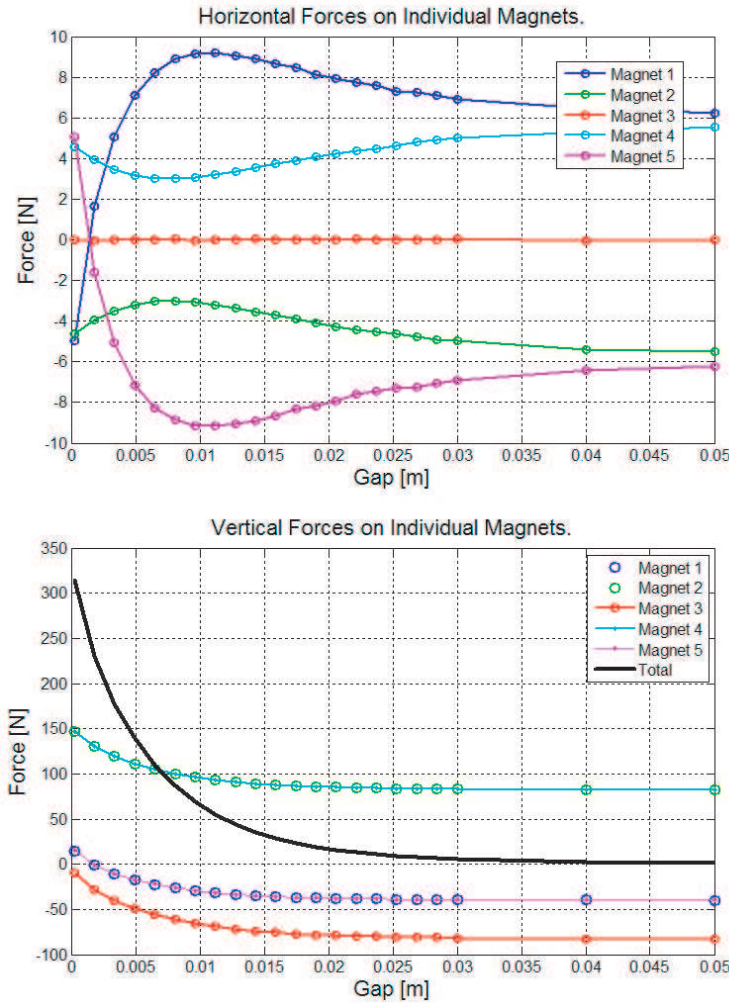
Figure 7. When two discretized Halbach arrays are compressed, as could be expected, there exists symmetry in the forces the different magnets experience. I.e., the outermost magnets experience the same horizontal forces, as the next outermost magnets do. Notice that for gap distances larger than approximately 4 cm, the vertical forces the individual magnets experience is only due to the other magnets in the Halbach array (i.e., only self-forces). These forces are manageable with adhesive glue.

The level of discretization (amount of individual magnets per wavelength) also affects the magnitude of the self-forces. The maximum and minimum of the vertical and horizontal forces that any magnet experiences in a single discretized Halbach array is shown below as a function of the number of magnets (the wavelength is still $L/2$). (Note that the length of the Halbach array is left unchanged. I.e., when increasing the discretization level the widths of the individual magnets decrease and the difference in the magnetization direction between consecutive magnets also decrease.) The total number of magnets in the array is $N + 1$ and, thus, for a discretization level of $N = 4$ (90° rotation between consecutive magnets) this corresponds to the case of a large gap distance in Fig. 7).

As seen in Fig. 8, in general, the self-forces diminish when the level of discretization increases (i.e., the difference in the direction of magnetic moment between consecutive magnets decrease). However, this is also due to the fact that the magnetic moment for each magnet decreases with increasing discretization as the size of the magnets decreases (with preserved magnetization properties of the material). The horizontal force for the case of $N = 4$ is an exception as then the magnetization directions are perpendicular between consecutive magnets.

See [20] for another reference on the self-forces and deformation in a (2D) Halbach array.
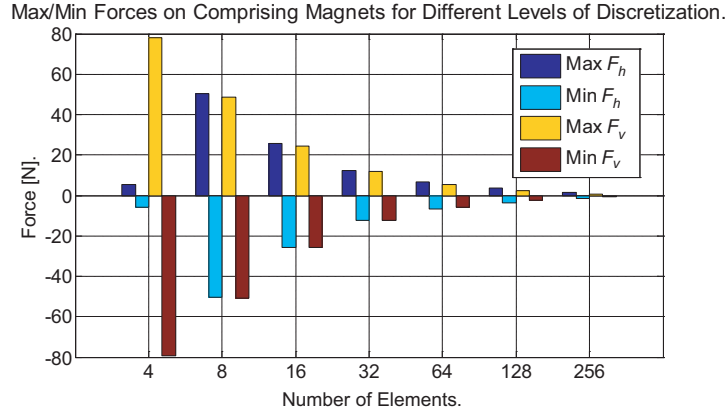
Figure 8. In general the maximum and minimum magnitude of the self-forces decreases as the discretization it improved. The exception being when the magnetic moment is rotated 90° between consecutive magnets.

5.3.2. Internal Forces in a Continuous Halbach Array

A continuous Halbach array (see Fig. 2) will also experience internal forces but these will be smaller. (Here only the self-forces are considered.) A better discretization of the discrete Halbach array (lower rotation angle for the magnetic moment) gives a smaller difference between subsequent magnets. From a rudimentary macroscopic approximation, this can be understood by looking at the torque a dipole magnet with magnetic moment $\bar{m}_i = m_0 \hat{z}$ experiences due to the consecutive (rotated) dipole magnet $\bar{m}_j$, producing a magnetic flux density $\bar{B}_j$. If $\bar{m}_i$ is in the $\hat{z}$ direction then the consecutive magnet is oriented in the "$\hat{z} + \hat{\varepsilon}$" direction. Thus, for a good discretization (i.e., approximately continuous) $\hat{\varepsilon} \approx 0$ and, thus, $\bar{m}_i \approx \bar{m}_j$. If both magnets are situated on the x-axis (and the physical dimensions of the dipoles are negligible), the torque becomes [17]:

$$\bar{N}_{i \leftarrow j} = \bar{m}_i \times \bar{B}_j \approx m\hat{z} \times \left(\frac{\mu_0}{4\pi r^3}\right) [3 (m_0 \hat{z} \cdot \hat{r}) \hat{r} - m_0 \hat{z}] = \left\{ \begin{array}{c} \hat{r} = \hat{x} \\ \hat{z} \cdot \hat{x} = 0 \\ \hat{z} \times \hat{z} = 0 \end{array} \right\} = 0 \qquad (7)$$

This can then be further applied to all consecutive magnets. The actual force will have some small finite value as a magnet will also experience a force from the other, non-neighboring magnets, but this effect will diminish the further away the influencing magnet is positioned.

(Alternatively, the force on $\bar{m}_i$ from $\bar{m}_j$ is, if $\bar{m}_i \approx \bar{m}_j$ $\bar{F}_{i \leftarrow j} = \nabla(\bar{m}_i \cdot \bar{B}_j) \approx 0$, as $\bar{B}_j \parallel m_i$ on the x-axis and $\bar{m}_i \cdot \bar{B}_j \Rightarrow$ constant inside the magnet with index i.)

5.3.3. Considerations of Material Strength

The mechanical properties, i.e., material strength, of the individual NdFeB magnets have to be taken into account. For a discretized Halbach array, with five NdFeB magnets each having a surface area of $1 * 1 \,\mathrm{cm}^2 = 100 \,\mathrm{mm}^2$ (each producing $1.3\,\mathrm{T}$), the maximum force that a magnet experience is at a gap distance of $250\,\mathrm{\mu m}$ and is in the order of hundreds of Newton (see Fig. 7 above). To be on the safe side we exaggerate and assume that a magnet experiences a force (in some direction) of $1\,\mathrm{kN}$ which gives a pressure of $10\,\mathrm{N/mm}^2$ ($10\,\mathrm{MPa}$). This pressure experienced is, in the energy storage configuration, still well below the limits [15] of the material strength of NdFeB (see Table 2).

Thus, the risk of shattering the individual magnets, from the magnetic forces, during compression is negligible/small. However, it should be noted that uncoated NdFeB magnets are highly susceptible to corrosion and can easily break [6]. Ferrite magnets are, however, insensitive to humidity and can be used, e.g., outdoors without special coating. (This is as the ferrite material is already in oxidized form, and can, thus, not oxidize any further.) Ferrite magnets, on the other hand, produce a much lower magnetic flux than magnets made of NdFeB. Magnets made of Samarium-Cobalt, SmCo, are less prone

Table 2. Measures of material strength for NdFeB (from [15]) and the, here, corresponding force limits for breakage.

Property	Value [N]	Limits [kN]
Flexural strength (N/mm^2)	250	25
Compressive strength (N/mm^2)	1100	110
Tensile strength (N/mm^2)	75	7.5

to corrosion and have a maximum energy product similar to NdFeB magnets, however, they are more brittle and "prone to cracking" according to supplier [21].

5.4. Impact on Efficiency from Eddy Currents in Surrounding Conductive Structures

When the magnets are moved during the compression, the flux in the environment changes with time and, thus, an electromotive force, $\varepsilon = -d\Phi/dt$, is created. This induces *eddy currents* (also called "Foucault currents") in any surrounding conducting material, e.g., metallic support structures. The faster the compression is, the larger the eddy currents are. According to Lenz' law, these currents are directed such that the magnetic flux density they in turn produce opposes the original change in the flux (i.e., "*nature abhors a change in flux*" quoting [17]). Thus, the magnetic flux density created by the eddy currents will, during compression, create an upward force on this magnet moving downward and a downward force on the magnet during release (i.e., utilization) of the potential energy. The consequence is that more force is needed to, e.g., compress the magnetic structures quickly than if done slowly.

The situation is similar to the case of a magnet falling in a conducting, but non-magnetic, tube, thus producing eddy currents that slow the fall (see Fig. 9).

This (see [22, 23]) is used as a model to estimate the decrease in efficiency during fast compression of the Halbach arrays. (Observe that the lower, stationary, magnet do not affect the creation of the eddy currents, and it is assumed that the speed of the moving, magnet is kept constant even though the force between the magnets increases.) In addition, it is assumed that the support structure of the Halbach arrays is a tube with conductivity σ (here $5.9 * 10^7$ S/m), inner radius a (here 2.5 cm) and thickness b (here 1 mm and assuming $b \ll a$). Therefore, when the upper magnet moves downward (with speed V)
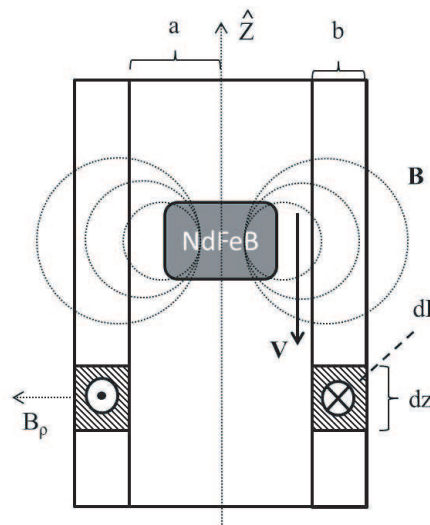

Figure 9. The compression of the Halbach arrays can be approximated by a magnet falling in a tube. When the magnet falls downward a current is created in the tube. This circulates in such a direction that the produced magnetic flux density opposes the increasing flux created by the magnet as it travels (i.e., "*Lenz Law*"). Thus, the journey of the free falling magnet is slowed.

an electromotive force is created accordingly to the changing flux:

$$\left.\begin{aligned} \varepsilon &= -\frac{d\Phi}{dt} = -\frac{d}{dt}\int \bar{B}\cdot d\bar{a} \\ d\bar{a} &= \left(\bar{V}\times d\bar{l}\right)dt \end{aligned}\right\} \varepsilon = \int \left(\bar{V}\times\bar{B}\right)\cdot d\bar{l}. \tag{8}$$

The cross product of the integral needs, for a non-zero contribution, to be in the φ direction (same direction as dl) and, thus, only the radial component of B (B_ρ) is of interest:

$$\left.\begin{aligned} \bar{V} &= -V\hat{z} \\ \bar{B} &= B_\rho\hat{\rho} \\ d\bar{l} &= ad\varphi\hat{\varphi} \end{aligned}\right\} \varepsilon = -2\pi aVB_\rho. \tag{9}$$

The induced eddy current, dI, along a ring, with resistance R, of the tube is:

$$dI = \varepsilon/R = \varepsilon\frac{\sigma da}{l} = \varepsilon\frac{\sigma bdz}{2\pi a} = -VB_\rho\sigma bdz. \tag{10}$$

Here it is assumed that the magnetic flux density of the Halbach array is dipole shaped (an acceptable approximation). It is not dipole shaped, but the difference compared to the actual magnetic field Halbach array will not influence the order of magnitude of the opposing force due to the eddy currents. We can then, from the magnetic flux density of a magnetic dipole (see Section 2), describe B_ρ in cylindrical coordinates (ρ, φ, z) as [23]:

$$B_\rho = \left(\frac{\mu_0}{4\pi}\right)\frac{3mz\rho}{(z^2+\rho^2)^{5/2}}, \tag{11}$$

where m is the magnitude of the magnetic dipole moment. This magnitude (m) is acquired from this as it can be seen that the field at a distance d above the dipole is $B = (\mu_0 m)/(2\pi d^3)$ (directed along the z-axis). Using FEMM to simulate a dipole with the same source magnitude $(1.03\,\mathrm{MA/m})$ as the individual NdFeB magnets investigated here, the value of m is found to be approximately $1.03\,\mathrm{A/m^2}$.

The vertical force dF_z on the magnet from the induced current element dI is:

$$dF_{\hat{z}} = dI\int \left(d\bar{l}\times B_\rho\hat{\rho}\right)_{\hat{z}} = -2\pi aB_\rho dI = 2\pi abV\sigma B_\rho^2 dz. \tag{12}$$

Thus, the total vertical force on the magnet from the entire tube (i.e., all of the induced eddy current along the tube) is upward and becomes (see [22, 23]):

$$F_{\hat{z}} = 2\pi abV\sigma\int_{-\infty}^{\infty} B_\rho^2 dz = \frac{36\pi b\sigma}{a^4}\left(\frac{\mu_0}{4\pi}\right)^2\frac{5\pi}{256}m^2 V. \tag{13}$$

In the analyses of the potential energy stored when compressing the Halbach arrays, the compression of the magnetic structures have been from a $5\,\mathrm{cm}$ distance to a $250\,\mathrm{\mu m}$ distance. If we assume that this is done in $1\,\mathrm{ms}$ (i.e., a very short charging time) the average speed of the downward traveling magnet is approximately $50\,\mathrm{m/s}$. The upward force, due to the eddy currents, on the magnet traveling downward at $50\,\mathrm{m/s}$ is then approximately only $0.5\,\mathrm{N}$. (Thus, the small error introduced by the dipole approximation is negligible.)

This force, and the work performed by the eddy currents on the magnet, is negligible compared to the force required for the compression (see Fig. 5). It should be noted that the time frames discussed for the compression (ms), corresponds to, an, approximately, maximum frequency for the currents created in the kHz range $(f_{\max} = 1/t)$. This is, thus, too low for skin effects to be of concern here.

Here, it was assumed that the support structure was a solid cylinder, but if it is segmented (vertically) with insulating material in between, the flow of the eddy currents is decreased, and the effect from these eddy currents are greatly mitigated. Also, a rod like support structure would remove the problem of eddy currents.

5.5. Temperature Impact

As already discussed (see Section 5.1), when the Halbach arrays are compressed the magnetic field inside the individual magnets increases. This increasing magnetic field gives rise to a generation of energy in the form of heat in addition to the potential energy already discussed. It is worth repeating that for, e.g., the N-graded NdFeB material the maximum working temperature (according to retailer [6]) is 80°C and the Curie temperature is 310°C for N-type material. If the temperature is increased above 80°C the magnets start to lose their magnetization and above the Curie temperature there is no remanence left.

Using [11, pp. 221, Eq. (5.169)] the heat generated in an individual NdFeB magnet, when two magnets are forcefully brought together once, can be estimated. A magnetic field of $1.5\,\mathrm{MA/m}$ is used, as this is well above the average magnetic field inside anyone magnet and also above the maximum field a magnet is exposed to (at the stopping distance of $250\,\mu\mathrm{m}$).

$$P_{res} = \frac{1}{2}\mu_0\mu_r\omega H_0^2 e^{-2z/\delta} \; [\mathrm{W/m^3}]$$

$$\left\{ \begin{array}{ll} \omega = \omega_{\max} \approx \dfrac{2\pi}{\Delta t} \; [\mathrm{rad/s}] & \mu_r = 1.05 \\ H_0 = 1.5 \cdot 10^6 \; [\mathrm{A/m}] & z = \delta \end{array} \right\} \Rightarrow \tag{14}$$

$$P_{tot} = P_{res}V \Rightarrow E_{tot}\Delta t \approx 1.2 \; [\mathrm{J}]$$

Aside from the potential energy stored, the heat generated for such an extreme magnetic field value is approximately $1.2\,\mathrm{J}$. (Please observe that this assumes that the total volume experiences a magnetic field of $1.5\,\mathrm{MA/m}$, which is an exaggeration. If the actual volume density for the magnetic field was used it is believed that the sum of the potential energy and the heat generated is closed to the $(B \times H)_{\max}$ of 318–$334\,\mathrm{kJ/m^3}$ already mentioned.)

To estimate the temperature increase from this $1.2\,\mathrm{J}$ we can use the expression below ([24]).

$$E_{tot} = \Delta Q$$

$$\Delta T = \frac{\Delta Q}{mC}$$

$$\left\{ \begin{array}{ll} \Delta Q = 1.2 \; [\mathrm{J}] & C = 0.5 \; [\mathrm{kJ/(kgC°)}] \\ m = \rho V = 7.4 \cdot 10^{-3} \; [\mathrm{kg}] & \end{array} \right\} \Rightarrow \tag{15}$$

$$\Delta T \approx 0.32 \, [\mathrm{C°}]$$

As can be seen the temperature increase is negligible. (However observe that this does not take into account heat transfer to and from the Halbach arrays via conduction, convection or radiation from the surroundings which have to be done for a complete analysis of the heating phenomenon in an operational system.) From this, it is also seen that the smaller the stopping distance between the magnets are to larger the magnetic field is inside the magnets. Thus, the heat generated increases with smaller stopping distance which should be taken into account for an operational system to keep the temperature below the operational temperature of the magnets (80°C for N-graded material) (especially if the outside temperature is relatively high or if the charge/discharge cyclic is frequently repeated).

In the support structure the heating will also exist due to the eddy currents but this will be smaller and can be minimized by segmenting the supporting structure.

6. COMPARISON TO OTHER ENERGY STORAGE MEDIA

Here, it is assumed that the efficiency of the auxiliary systems required for operation (e.g., motors, gear boxes etc.) are of equal performance to those auxiliary systems used by other energy storage systems (by e.g., flywheels). It can be difficult to find reliable data on commercial or operating energy storage systems as available material often do not refer to published scientific sources. However, published scientific studies exist. For example, in flywheels where the energy is stored in the inertia of a rotating mass (as kinetic energy) it is seen ([25]) that the mass energy density can reach, depending upon the shape and material strength of the flywheel, $32\,\mathrm{kJ/kg}$. Data on other energy storage systems is found in [1–3] (see Table 3).

Table 3. Data on some energy storage systems (adopted from [1]).

Type	Energy density (J/m^3)	Charge time (s)
Flywheel	10^8	0.1
Pumped hydro	10^6	10
CAES[1]	10^5	360
TES[2]	10^9	"Tens of minutes"
Batteries	/	0.01
Capacitor	/	0.01
SMES[3]	/	0.01

[1]Compressed air energy storage.
[2]Thermal energy storage.
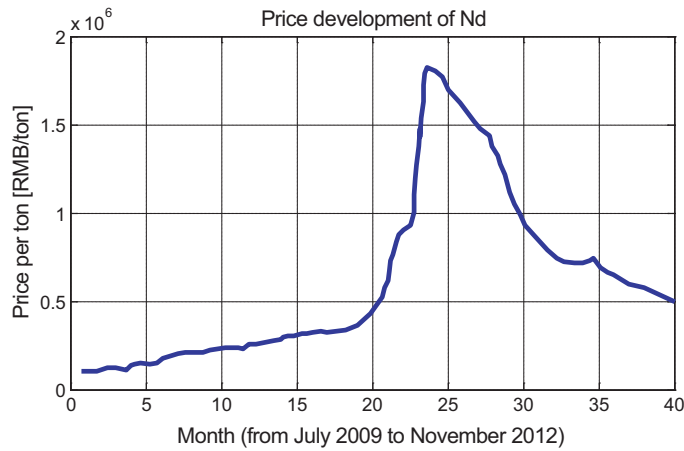[3]Superconducting magnetic energy storage.

Figure 10. The price development of neodymium (adopted from [6]).

Looking at the mass- and volume energy of the Halbach units (32 J/kg and 241 kJ/m^3) these are in general lower than other energy storage systems (only comparable with CAES (compressed air energy storage)). However, as can be seen the charge/discharge times for existing systems are, longer (between 0.01 s to "tens of minutes" (similar results are found in [3])) compared to what is judged possible for the Halbach energy storage system (1 ms). Data on discharge times can also be found here [26].

In addition, the high cost of NdFeB is also a large disadvantage. The 1 cm^3 NdFeB magnets used here can be bought [6] for approximately 0.5 € per magnet. In our example the two Halbach arrays stored approximately 2.4 J with 10 such 1 cm^3 magnets. This leads to a cost of $10*0.5$ € $/2.4$ J ≈ 2.1 €/J (≈ 2.9 USD/J) which is ineffective if compared to, e.g., flywheels, 0.28 USD/kJ (1000 USD/kWh) [26]. Also, restrictions on the export of such rare earth materials have made the price fluctuate in the past (see Fig. 10). The large cost is mainly due to the dominant mining operation of the rare earth materials, which is today located in China.

However, attempts to create permanent magnets free of rare-earth elements [27] exist and cost of permanent magnets might thus change. Ferrite magnets could be used, but the energy stored would be, for the same configuration, less.

Observe that the power density of the Halbach array is not directly discussed here. This as the speed of the compression or release of the stored energy affects this and this is dependent on the ancillary equipment which is not discussed here. However as we have seen the speed of the compression/release do not to any degree affect the Halbach array detrimentally.

7. CONCLUSION

Disregarding auxiliary equipment, it was seen that the limiting phenomena (eddy currents in support structure, internal mechanical stresses, temperature increase, and demagnetization risk) do not significantly affect the performance. Thus, one possible application could be energy storage systems were the main critical aspect is not the energy density of the storage medium but very fast charge/discharge times with repetitive cycles and good charge/discharge depth. Fast changes in the load curve can lead to instabilities in the power grid and thus a fast energy storage system can mitigate this [2]. Otherwise, due to the high cost of NdFeB magnets this makes the Halbach array unsuitable as a wide spread common potential energy storage medium.
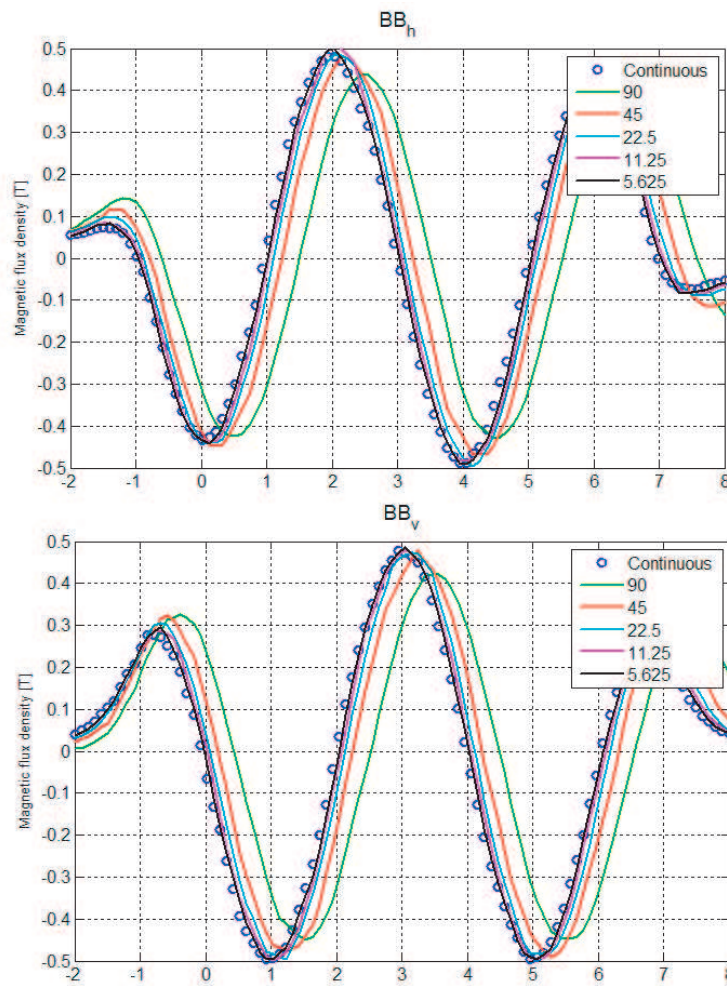
APPENDIX A.

Figure A1. Shown are the horizontal and vertical component of the magnetic flux density for different degree of discretization taken through a line 1 cm away from the Halbach array. Below approximately 20° the difference, between a continuous and discretized Halbach array, is negligible and at (approximately) 6° it is undetectable.
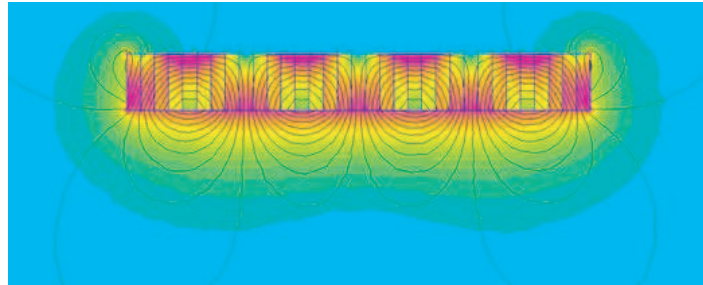
Figure A2. The magnetic flux density from a discretized Halbach array (22.5° rotational angle on the magnetization direction), compare to Fig. 2 (the continuous Halbach array).

REFERENCES

1. Ter-Gazarian, A. G., *Energy Storage for Power Systems*, 2nd edition, The Institution of Engineering and Technology, London, 2011.

2. Huggins, R. A., *Energy Storage*, Springer Science + Business Media, New York, 2010.

3. Rosen, M. A. (Ed.), *Energy Storage*, Nova Science Pub Inc., Hauppauge, 2012.

4. Grijalva, S. and M. U. Tariq, "Prosumer-based smart grid architecture enables a flat, sustainable electricity industry," *IEEE PES Innovative Smart Grid Technologies (ISGT)*, 2011.

5. Zheng, J., D. W. Gao, and L. Li, "Smart meters in smart grid: An overview," *IEEE Green Technologies Conference*, 2013.

6. Supermagnete, Available: http://www.supermagnete.de/eng/.

7. Pawlowski, M., "Permanent magnet energy storage apparatus," U.S. Patent 5446319 A, August 29, 1995

8. Finite Element Method Magnetics, Available: http://www.femm.info/.

9. Meeker, D., "Force on a taper plunger magnet," Available: http://www.femm.info/wiki/RotersExample.

10. Vizimag, Available: http://www.softpedia.com/get/Science-CAD/Vizimag.shtml.

11. Jackson, J. D., *Classical Electrodynamics*, 3rd Edition, John Wiley & Sons Inc., Hoboken, 1999.

12. Mallinson, J. C., "One-sided fluxes — A magnetic curiosity?," *IEEE Trans. Magnetics*, Vol. 9, 678–682, 1973.

13. Halbach, K., "Physical and optical properties of rare earth Cobalt magnets," *Nuclear Instruments and Methods in Physics Research*, Vol. 187, 109–117, August 1981.

14. Post, R. F. and D. D. Ryutov, "The inductrack approach to magnetic levitation", *MAGLEV 2000 The 16th International Conference on Magnetically Levitated Systems and Linear Drives*, Rio de Janeiro, Brazil, June 6–11, 2000.

15. Pyrhönen, J., T. Jokinen, and V. Hrabovcová, *Design of Rotating Electrical Machines*, John Wiley & Sons, Hoboken, 2009.

16. Friend, P., "Magnetic levitation train technology 1," *Tech. Rep.*, Department of Electrical and Computer Engineering, Bradley University, May 2004.

17. Griffiths, D. J., *Introduction to Electrodynamics*, 3rd Edition, Prentice-Hall Inc., Upper Saddle River, 1999.

18. Ma, G. T., J. S. Wang, and S. Y. Wang, "3d finite element modeling of a Maglev system using bulk high Tc superconductor and its application," *Applications of High-Tc Superconductivity*, A. Luiz (ed.), InTech, Available: http://www.intechopen.com/books/applications-of-high-tc-superconductivity.

19. Sakamoto, T. and H. Wakimoto, "Internal stress analysis of Halbach array magnets with application to linear synchronous motors," *International Symposium on Power Electronics, Electrical Drives, Automation and Motion, 2008, SPEEDAM 2008*, 136–141, June 11–13, 2008.

20. Rovers, J. M. M., J. W. Jansen, E. A. Lomonova, and M. J. C. Ronde, "Calculation of the static forces among the permanent magnets in a Halbach array," *IEEE Trans. Magnetics*, Vol. 45, No. 10, October 2009.

21. Magpole, Available: http://www.magnetpole.com/smco-magnets-71.html.

22. Donoso, G., C. L. Ladera, and P. Martín, "Damped fall of magnets inside a conducting pipe," *Am. J. Phys.*, Vol. 79. No. 2, February 2011.

23. Donoso, G., C. L. Ladera, and P. Martín, "Magnet fall inside a conductive pipe: Motion and the role of the pipe wall thickness," *Eur. J. Phys.*, Vol. 30, 855–869, 2009.

24. Beckman, O., G. Grimvall, B. Kjöllerström, and T. Sundström, *Energilära — grundläggande termodynamik*, Solna, Liber, 2005.

25. Arslan, M. A., "Flywheel geometry design for improved energy storage using finite element analysis," *Materials & Design*, Vol. 29, 514–518, 2008.

26. Electricity storage association, Available: http://www.electricitystorage.org/technology/storage_technologies/technology_comparison.

27. "Rare-earth free permanent magnets," Available: http://refreepermag-fp7.eu/project/what-is-refreepermag/.